Block Copolymer Micellisation in a Common Solvent Modeled by Self-Consistent Field Calculations

Frans A. M. Leermakers

Summary: Recently it was shown that it is possible that block copolymers form micellar solutions in non-selective solvents. Such micellisation is the result of a pure form of self-assembly. A molecular realisation is given by asymmetric Poly-(methacrylic acid)-*block*-Poly(ethylene oxide) copolymers (PMAA-*b*-PEO) in water at a pH < 5. As both the (short) methacrylic acid block and the (long) ethylene oxide are water soluble in the conditions used, it was concluded that the driving force is interchain hydrogen bonding between the PMAA and the PEO units. The mismatch in length of the blocks forces one block to accumulate at the micellar periphery and this eventually stops the phase separation process. We have performed self-consistent field calculations to examine this scenario. With very reasonable parameters we are able to mimic the properties of these micelles, elaborate the pH dependence and confirm the trend found for the electrophoretic mobility. A nontrivial result of the calculations is that the ratio EO/MAA in the core is close to two.

Keywords: block copolyer self-assembly; modeling

Introduction

The topic of polymer self-assembly is high on the scientific agenda for many good reasons. The formation on nanoscale objects without external energy input is the way to go in bottom-up nanotechnology. Similarly as is known for the self-assembly of surfactants in aqueous solutions[1] it is usually easy to identify a driving force for the assembly[2] Classically the driving force is a demixing of one part of the copolymer with the solvent, similarly as the demixing of hydrocarbon tails and water. Equally important for the thermodynamic stability of micelles is a stopping force. Without a stopping mechanism only macroscopic demixing can be found: oil and water don't mix.

In surfactants the head group accumulates on the outside of the micelle and the pressure built-up of overlapping and strongly interacting head groups inhibits further increase of the aggregation number.[1] n polymeric systems the same strategy is used. One of the blocks has the role of the head group. This block accumulates in a corona around the core. Upon an increase of the aggregation number (that is the increase in the number of copolymers in the micelle), the corona chains begin to overlap and then become strongly stretched; there is a built-up of a polymer brush.[3–8] As soon as all the energy gain of the block that forms the core is needed to stretch the chains in the corona the growth of the micelles comes to a hold.[9–11] Micellisation in copolymeric as well in surfactants systems thus typically occurs when the solvent is selective: it must be poor for one block (chain fragment) and good for the other.

One is inclined to think that this scenario must be underneath all types of micelle formation. Indeed, one should always be able to identify a starting and stopping mechanism for the formation of mesoscopic objects. However, there can be surprises. Clearly, in the field of polymer self-

Laboratory of Physical Chemistry and Colloid Science, Dreijenplein 6,6703 HB Wageningen,Wageningen University, The Netherlands
E-mail: frans.leermakers@wur.nl

assembly there are ways to significantly deviate from the sketched scenario.

Recently it was shown that micellisation proceeds without the presence of a selective solvent, i.e., it occurs in a common (good) solvent for all blocks. For example, in the case of two oppositely charged and thus soluble polyelectrolytes one can form an interpolyelectrolyte complex that in turn may not be soluble in water. The precipitate is sometimes referred to as a complex coacervate, especially when it is liquid like.[12]

This phase behavior can be exploited to form micelles by introducing a neutral block in one or in both of the chains. In this case the complex coacervate forms the core of the micelle and the neutral block will automatically accumulate in the corana. The micelles are known as Complex Coacervate Core Micelles or C3M's.[13,14] The C3M's are most stable when the number of charges that the oppositely charged polyelectolytes contribute to the micelle is the same, i.e., at equal stocheometric conditions. This type of assembly may be called obligatory co-assembly because it is necessary that two soluble species come together to form the micelles. Surprisingly C3M's can exists up to reasonably high ionic strength.[15]

Recently it was shown that it is also possible to form micelles by adding to a 'polyelectrolyte'-*b*-'neutral' copolymer a combination of a (small) bisligand molecule and a suitable metal ion.[16] Due to the complexation of the bisligand with the metal ions linear chains (and rings) can form which appear to have (locally) some excess charge (depending on the type of metal ion used). These association polymers can make an inter-polyelectrolyte complex with the block polyelectrolyte to form micelles with a core loaded with metal and bisligand. In these micelles we thus recognise two independent mechanisms of assembly.[16] On the one hand it is the formation of living chains by the head-tail coupling of the bisligand with the metal and on the larger scale the association polymers combine with the copolymers and form micellar species.

Micelle formation in a common solvent thus seems to require the presence of at least two types of molecules. Upon the interaction of these two molecules a complex is formed for which water appears to be a poor solvent. In this sense the system returns to the classical self-assembly case of a block copolymer in a selective solvent. The formation of micelles due to the attractive nature of opposite charges is not the only non-classical mechanism to assemble micelles. Multiple hydrogen bonding is also possible, albeit that in water the intrachain H-bonds must compete H-bonds with water. This mechanism is perhaps only feasible in polymeric systems where the cooperativity of long chains can be exploited.

Recently, Konak and Sedlak[17] reported the finding that poly(methacrylic acid)-*b*-poly(ethylene oxide) PMAA-PEO copolymers are able to form micelles (with a size above 30 nm) in acidic aqueous solutions. In this paper the authors show that both blocks are water-soluble at the conditions used. This means that even though the poly(Methacrylic acid) block is weakly charged, it remained completely soluble in water. Also the poly(Ethylene oxide) is soluble in water around room temperature. Clearly in this system the solvent is not selective. As there is just one type of copolymer in the system, there is no possibility of coassembly either.

The authors propose that there is inter- and intra molecular H-bonding which is the driving force for the formation of the micelles. The oxygen of the EO units is a proton acceptor while the proton on the PMMA units can be used for the H-bond. Indeed mixtures of sufficiently long PMAA and PEO do make a complex which subsequently expels water, i.e., they form a precipitate.[17] To form stable micelles, however, it is then necessary to have a significant mismatch in lengths of the copolymer. The longest block will then accumulate at the outside of the micelles forming a corona. In line with the proposed mechanism the authors showed a strong dependence of the micelle size on the pH.

There are two reasons for the pH sensitivity. Firstly, with increasing pH the PMAA block becomes deprotonated and thus has less protons for the inter-chain H-bonding. Secondly the charge-up of the corona will attract counter-ions and water into the core which destabilises it.

In this paper we report self-consistent field modeling of micelles composed of asymmetric copolymers with one chargeable block and another block that can form H-bonds with the protonated core-forming block. The target of the investigations is to underpin the proposed mechanism of micellisation and to evaluate the internal structure of these micelles.

Self-Consistent Field Theory and its Parameters

Here we employ the self-consistent field theory using the Scheutjens and Fleer discretisation scheme (SF-SCF).[18] Initally used to describe polymers at interfaces, it was found that this model is ideally suited to study self-assembly.[19–30] Details of this method are readily available in the literature, and we refer to the references just mentioned. Below we will pay attention to the most important features, while we introduce the parameters in the model. Parameters are coupled to the coordinate system used (i.e. the lattice), the molecules in the system and the monomeric species. In the current problem we account both for electrostatic as well as short-range interactions.

The Lattice

A spherical coordinate system is used with concentric layers of lattice sites numbered $r = 0, 1, 2, \ldots$. The number of lattice sites in each layer grows roughly quadratic with the layer number, i.e., $L(r) \sim r^2$. The center of mass of the spherical micelle will be at $r = 0$. The last layer in the system $r = M$ is far outside the micelle and all gradients in density and electrostatic potential have died out. Nevertheless reflecting (mirror-like) boundary conditions are imposed between layers $r = M$ and $r = M + 1$. For very large values of r the *a priori* step probability to go from layer r to a next layer $r + 1$, $\lambda(r,r+1)$ is given by the value of a cubic lattice, i.e. goes towards the limiting value 1/6. For small values of r the internal balance equation applies $L(r)\ \lambda(r,r+1) = L(r+1)\ \lambda\ (r+1,r)$. The volume of the simulation box is $V = 4/3\ \pi\ M^3$ in units of lattice volumes $v_0 = b^3$. We note that all linear lengths are normalised by the lattice length $b = 6\ 10^{-10}$ m, close to the Bjerrum length.

The Molecules

In the system we have four different molecular species, which are numbered, $i = 1, \ldots, 4$.

$[i = 1]$ The first species is a block copolymer $A_{N(A)}$-$EO_{N(EO)}$. Here and below we will qualitatively follow the experimental system[17] and thus we consider the case that the length of the EO part exceeds that of the acid block. More specifically we take $N_A = 100$ and $N_{EO} = 400$. The acid groups have two states, $k = 1,2$. The neutral state $k = 1$ and the state with a single negative charge $k = 2$. The EO units are assumed to have just one single state. The number of copolymers in the system volume is adjusted to generate a for each condition (pH) a complete set of micelles. A thermodynamic criterion is used to select the relevant micelle.

$[i = 2]$ The monomeric solvent will be referred to as water. The normalisation of the water distribution is taken such that in the bulk (that is far from the micelle) all lattice sites are filled by molecular species. Water has three internal states ($k = 1,2,3$). The neutral state ($k = 1$) is in equilibrium with the protonated state ($k = 2$) and the deprotonated state ($k = 3$) according to an autodissociation reaction (see below).

$[i = 3]$ A monomeric negative co-ion. Generically referred to as Cl^-. The concentration of the bulk is fixed to $\varphi^b_{Cl} = 10^{-3}$

which corresponds to approximately $c_s = 10^{-2}$ M.

[$i = 4$] A monomeric positive counterion. Generically referred to as Na^+. The concentration of this ion is adjusted such that the bulk becomes electroneutral. As the concentration of the polymeric species in the bulk is very low, the negative charge due to the polymer in the bulk is small compared to that of Cl, and thus $\varphi^b_{Na} \sim \varphi^b_{Cl}$.

Multi-State Monomers and Their Reaction Equilibrium

There exists two species with multiple state.

[Water] The reaction equilibrium $2\ H_2O \leftrightarrow H_3O^+ + OH^-$, is implemented with a a dimensionless reaction constant $pK_W = 16$ (corresponding to classical value $pK_W = 14$). The volume fraction of protons in the bulk is an input parameter which is directly linked to the pH. Below we will report the pH values used in all cases.

[Acid] For the acidic groups of the copolymer there exits the reaction $A + H_2O \leftrightarrow A^- + H_3O^+$, where on the left hand side we have the segment A in state $k = 1$ and on the right hand side it is in state $k = 2$. The reaction constant for this reaction is fixed to the dimensionless value $pK = 5.5$ which corresponds to $pK_A \sim 4.5$ when it is transformed in the usual units ($\varphi_W = 1$ corresponds to approximately 10 mol/L -this depends on the lattice pararmeter b-). Details can be found in ref. [31].

The Interactions

As some of the species are charged we need to solve the Poisson equation. In the present case there are no hydrophobic species and therefore it is reasonable to fix the dielectric permittivity throughout the system to that of water. Hence, $\varepsilon_r = 80$ throughout the system. For each coordinate we compute the excess charge by:

$$q(r) = e[\varphi_{Na}(r) + \varphi_{W2}(r) - (\varphi_{A2}(r) + \varphi_{W3}(r) + \varphi_{Cl}(r))] \quad (1)$$

where e is the elementary charge. This charge distribution is inserted into the Poisson equation to obtain the electrostatic potential profile $\psi(r)$ in the system.

$$\frac{2}{r}\frac{\partial\psi(r)}{\partial r} + \frac{\partial^2\psi(r)}{\partial r^2} = -\frac{q(r)}{\varepsilon_0\varepsilon_r} \quad (2)$$

where ε_0 is the dielectric permittivity of vacuum.

Segments of type X that carry a charge with valency υ_X have an electrostatic contribution to their segment potential $u^{el}_X(r) = e\upsilon_x\psi(r)/k_BT$ where k_BT is the thermal energy. Besides this electrostatic contribution there are short-range interactions that are accounted for on the Bragg-Williams level,

$$u^{BW}_X(r) = k_BT\sum\nolimits_Y \chi(X,Y)\left(\langle\varphi_Y(r)\rangle - \varphi^b_Y\right) \quad (3)$$

where $\chi(X,Y)$ the familiar FH interaction parameter between segments of type X and Y. The following interactions were used. $\chi(W,EO) = 0.4$ mimicking slight better than theta solvent for EO units. $\chi(W,A) = 0.6$. This slightly worse than theta is very close to but below the critical interaction above which A_{100} chains can precipitate. We need this value to make the PMAA block only barely soluble. Except for $\chi(EO,A_1) = -2$, all other parameters are set to theta conditions, i.e., $\chi = 0.5$. The strongly negative value for $\chi(EO,A_1)$ drives the micelle formation. With this value we mimic the fact that the protonated state of the A's interacts favorable with the EO's. Although we envision that this is due to the formation of H-bonding, we here mimic this by a negative FH value.

In Equation (3) the angular brackets indicate a three-layer average of the volume fraction according to

$$\langle\varphi(r)\rangle = \lambda(r,r-1)\varphi(r-1) + \lambda(r,r)\varphi(r) + \lambda(r,r+1)\varphi(r+1) \quad (4)$$

The total segment potential reads $u_X(r) = u'(r) + u^{BW}_X(r) + u^{el}_X(r)$. In this segment potential $u'(r)$ is a Lagrange field

coupled to the incompressibility condition $\sum_X \varphi_X(r) = 1$.

Markov Chains

All possible and allowed chain conformations are generated and their statistical weight added, resulting in the radial volume fraction profiles. For all monomeric species X' this procedure simplifies to the Boltzmann equation

$$\varphi_{X'}(r) = \varphi^b_{X'} G_{X'}(r) = \varphi^b_{X'} \sum_k \alpha^b_k \exp\frac{-u_{X'}(r)}{k_B T} \quad (5)$$

which defines the so-called free segment distribution function $G_X(r)$. Here α^b_k is the probability that the segment (in the bulk) is in internal state k. Of course for segments that have just one state $k = 1$ we have $\alpha^b_1 = 1$. For the other segments that have multiple states one can compute the α^b_k values from the pK_W, the pH and the pK_A values. For the copolymer with segment ranking number $s = 1, \ldots, 500$ we introduce $\delta(s,A) = 1$ for $s < 101$ and zero otherwise and $\delta(s,EO) = 1$ for $s > 100$ and zero otherwise. Using this we find the ranking number dependent free segment distribution functions $G(r,s) = \delta(s,A)\ G_A(r) + \delta(s,EO)\ G_{EO}(r)$ for all segments s. For the segments in the chain the volume fractions follow from

$$\varphi(r,s) = \frac{\sigma}{Q} G(r,s|1) G(r,s|500) / G(r,s) \quad (6)$$

where σ is the number of copolymers in the system, $Q = \sum_r L(r) G(r,500|1)$ is the single-chain partition function. Further, Equation (6) features a pair of end-point distribution functions which basically obey to the Edwards diffusion equation.

$$\frac{\partial G(r,s|s')}{\partial s} = \frac{1}{6}\left(\frac{2}{r}\frac{\partial G(r,s|s')}{\partial r} + \frac{\partial^2 G(r,s|s')}{\partial r^2}\right) - u(r,s) G(r,s|s') \quad (7)$$

where $s' = 1$ or $s' = 500$ are the two initial conditions used (initial conditions are: $G(r,1|1) = G(r,1)$ and $G(r,500|500) = G(r,500)$ for all r). On a lattice this equation simplifies to a propagator equation which gives direct access to all $G(r,s|1)$ and $G(r,s|500)$ values. In this propagator formalism the Edwards equation maps onto a freely-jointed chain model.[18]

Using $\varphi_A(r) = \sum_s \delta(s,A)\varphi(r,s)$ and $\varphi_{EO}(r) = \sum_s \delta(s,EO)\varphi(r,s)$ gives access to the volume fraction profiles of the polymeric units. The distribution of the charged component may be found by $\varphi_{A2}(r) = \alpha_{A2}(r)\varphi_A(r)$ where the local degree of dissociation is found by $\alpha_{A2}(r) = \alpha^b_{A2} G_{A2}(r)/G_A(r)$. For the water components similar equations apply: $\varphi_{Wk}(r) = \alpha^b_{Wk} G_{Wk}(r)/G_W(r)$ for all three states of water.

Numerics

The above set of equations is solved routinely on a PC up to seven significant digits. Details can be found elsewhere.[32] For such a solution it is true that the volume fractions both determine and follow from the segment potentials and *vice versa*.

For such SCF solution it is possible to extract structural information, such as measurable radial distribution functions and thermodynamic quantities. As will be discussed in the next section the grand potential of a micelle ε_m is a central quantity. It is found straightforwardly once the volume fraction and the segment potential profiles are known. We refer to the literature for details.[32]

Thermodynamics of Small Systems

In the SCF model one can generate micelles of various aggregation number. As told already all micelles have their center of mass at the center of the coordinate system and thus these micelles have no

translational degrees of freedom. Typically these translationally-restricted micelles have a grand potential ε_m that is non-zero. From classical thermodynamics it follows that equilibrium micelles should have a vanishing grand potential $\varepsilon = 0$.[33] We thus conclude that the grand potential as found for the micelle ε_m) in the SCF calculations should be matched with the contribution due to translational entropy, i.e., in dilute solution by $k_BT \ln \varphi_m$, where φ_m is the volume fraction of micelles. This results in

$$\varphi_m = \exp\frac{-\varepsilon_m}{k_BT} \tag{8}$$

As the volume fraction of micelles must be less than unity we conclude that $\varepsilon_m > 0$. Moreover, the micelle concentration increases with decreasing value of ε_m. It can be shown that for the SCF system there exists a Gibbs Duhem relation

$$\frac{\partial\varepsilon_m}{\partial\mu} = -g \tag{9}$$

where g is the aggregation number of copolymers in the micelle and μ is the chemical potential of the copolymers (note that the chemical potentials of the ions are fixed). The aggregation number g is computed from the volume fraction profile of the polymer $\varphi(r) \equiv \varphi_1(r)$ by elvaluating the excess amount in the micelle:

$$g = \frac{1}{500}\sum_t L(r)\left(\varphi(r) - \varphi^b\right) \tag{10}$$

The fluctuations in micelle size are found by $\sigma_g^2 = k_BT\partial g/\partial\mu$. This quantity necessarily must be positive. We conclude that $\partial\varepsilon_m/\partial g < 0$. Hence the micelles grow with increasing micelle concentration. All these results are consistent with experimental findings and are well-known results for micellar solutions.[1] We note that for polymeric systems with polydisperse size distributions an anomalous increase in micelle size with decreasing concentration is possible. We do not go into these details here.[17,32]

Results and Comparison to Experimental Data

The SCF calculations show that micelles composed of block copolymers where one block is a good proton donor and the other block is a proton acceptor are thermodynamically feasible. In Figure 1 the grand potential is plotted as a function of the aggregation number g for a number of relevant pH values. As explained above for thermodynamic stability we need positive values for ε_m and a negative slope, i.e. $\partial\varepsilon_m/\partial g < 0$. This indeed occurs in these systems for aggregation numbers consistent with experimental findings. It is important to notice the strong pH dependence for a pH slightly lower than the corresponding pK_A of the MAA groups (which is pK = 4.5). Below pH = 3 there is a very weak dependence, basically because all PMAA groups are fully protonated and the micelles carry very few charges. The ionic strength is also unimportant for this case. Above pH = 3, and especially near pH = 4 the changes are dramatic. In fact above pH = 4.1 we failed to find stable micelles any longer. In line with the report

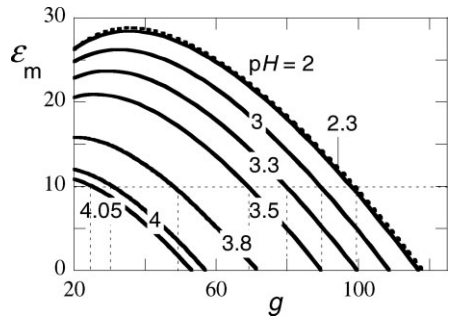

Figure 1.
The grand potential ε_m (in units of k_BT) of micelles frozen to the center of the coordinate system as a function of the aggregation number g for various values of the pH as indicated. The horizontal dotted line at $\varepsilon_m = 10\ k_BT$ is indicating micelles around a measurable concentration (near the experimental CMC). The vertical dotted lines point to the corresponding aggregation numbers. The line for pH = 2 is dotted so that it is possible to appreciate the difference with the curve for pH = 2.3. All other parameters are have their default value.

in ref. 17 it is thus impossible to find micelles as soon as the average degree of dissociation of the MAA groups exceeds roughly 30%.

The physical interpretation of the grand potential as plotted in Figure 1 is standard. It is directly coupled to the micelle volume fraction ε_m (cf Equation (8)). The maximum in the $\varepsilon_m(g)$ curve corresponds to the smallest stable micelles, i.e. micelles at the theoretical CMC. These smallest micelles however typically occur at extremely low micelle concentration. It is often impossible to observe these experimentally. The horizontal dotted line at $\varepsilon_m = 10\ k_BT$ represents the case where the micelle volume fraction amounts to $\varphi_m \sim 10^{-5}$. Such concentrations may be seen by, e.g., scattering techniques. Already from Figure 1 we can see that these observable aggregation numbers are a very strong function of the pH.

The pH dependence of both the aggregation number as well as the CMC is presented in Figure 2. Here the CMC is defined as the bulk volume fraction of copolymers with which the first micelles are in equilibrium with. As is seen from Figure 2a the aggregation number is stable at low pH and then very quickly vanishes just above pH = 4. Experimentally[17] it was found that the mass of the micelles dropped to zero around pH ~ 4.5 and that at pH = 4 the molar mass was three times less than that at pH = 3.5. Our results are in excellent agreement with these data (even quantitatively). In ref 17 results were presented for pH < 3.5. For this reason it is impossible to confirm the leveling off of the aggregation number at low pH values.

The CMC as presented in Figure 2b, is an extremely strong function of the pH as well. Experimentally a relatively high CMC is reported,[17] but the pH dependence was not discussed. Our predictions give a possible reason for this; the CMC becomes simply too low. We note that compared to polymeric micelles in strongly selective solvents, the CMC of the present micellar systems is relatively high.

Even though experimentally there is not much information yet about the detailed structure of the micelles, we nevertheless may pay some attention to this. In Figure 3a,b we show a pair of radial volume fraction profiles for the two blocks of the copolymer for relevant micelles at the extreme pH values used in Figure 1, namely pH = 2 and pH = 4.05. There is a number of interesting issues to be discussed about the structure of these micelles. First of all we see that the micelles have a well-defined core, where all the MAA segments are located. The PEO fragments are both in the core as well as in the corona. The polymer density profiles in the core are basically flat. This is identical to classical micelles formed in a selective solvent. Interestingly the stocheometry of PEO/MAA deviates significantly from unity. Inspection shows that this ratio is approximately two for all micelles generated, albeit that it increases with decreasing pH. The insensitivity of the overall polymer density with pH is

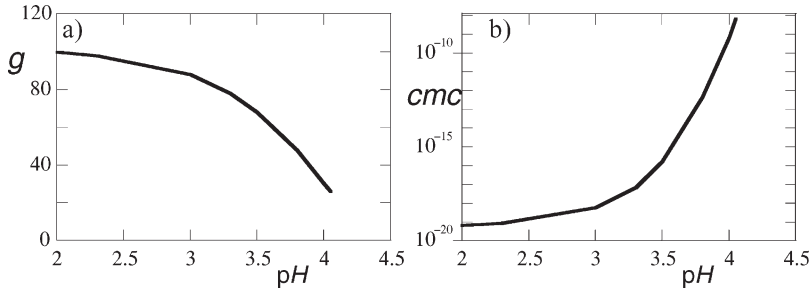

Figure 2.

a) The aggregation number g as a function of pH, b) the CMC (on logarithmic scale) as a function of pH. Data taken for micelles with grand potential $\varepsilon_m = 10\ k_BT$. All parameters as in Figure 1.

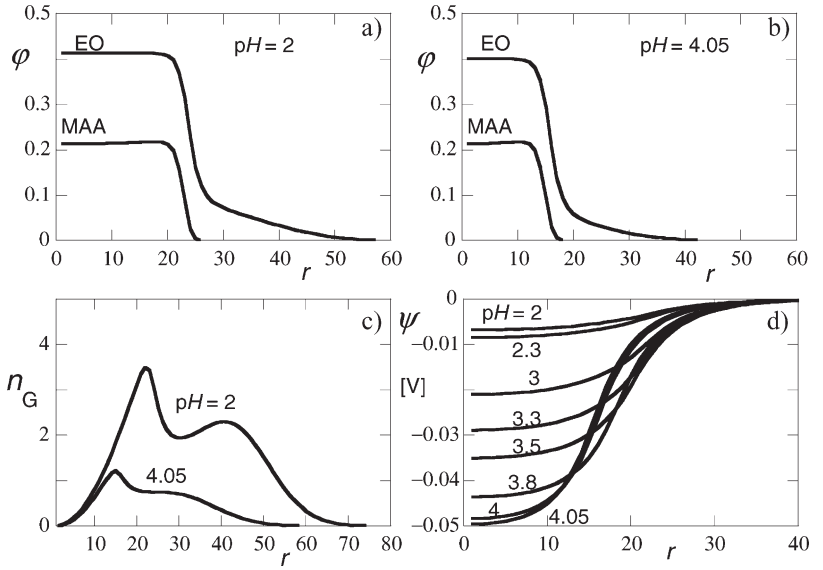

Figure 3.
a) Radial volume fraction profiles for the EO and the MAA segments as indicted for pH = 2. b) Radial volume fraction profiles profiles for the EO and the MAA segments for pH = 4.05. c) The number of end-points of the EO block as a function of the distance r from the surface for pH = 3 and 4.05 as indicated. d) The radial electrostatic potential profiles (in Volts) for the micelles at the pH as indicated. The micelles for which these properties are given all have a grand potential $\varepsilon_m = 10\ k_BT$.

surprising because with increasing pH the core becomes gradually more charged. Possibly this insensitivity is somewhat related to our parameter choices: for simplicity we have taken the ions to have similar properties as the solvent molecules.

The higher the number of EO-MAA contacts the better it is for the stability of the core. This optimum number not necessarily occurs at stocheometry. The increase in EO in the core may increase the number of MAA-EO contacts (H-bonds). Increasing the EO contents, however, increases the crowding. With increasing aggregation number gradually more EO is expelled (due to the crowding) from the core. As a result, the corona is exclusively composed of PEO chain-parts. These chains become strongly stretched and have the quasi planar brush volume fraction distribution. The quasi-planer profile is expected because the micelle core size is not much smaller than the size of the corona in these cases.[26]

We have labeled the end of the PEO block and this end is referred to by the letter G. In Figure 3c we give the distribution of chain ends. Plotted is $n_G(r)$ which is the number of ends at a distance r from the center. The distribution of ends is of particular interest, because it gives insight in some basic question about the conformations of the EO block. Basically there are two options. (i) All PEO blocks are partly in the core and partly in the corona. (ii) Some chains are fully in the core and others are completely in the corona. As concluded from Figure 3c the end-point distribution is bimodal (especially for low pH values). This clearly points to the second scenario. Some chains ends are in the core and others are far from the core.

The end-point distribution may also be used to estimate the hydrodynamic radius of these micelles. Indeed, what radius is measured for these micelles by dynamic light scattering is uncertain, but going from pH = 2 to pH = 4.05 results in a modest shift

of the maximum of the end-point distribution from approximately $R_h = 42b$ (~25 nm) for pH = 2 to $R_h \sim 27b$ (~16 nm) at pH = 4.05 (just before the micelles fall apart). In the experiments[17] a drop of the hydrodynamic radius from close to 35 nm at pH = 3.5 to approximately 22 nm at pH = 4 was reported. These data suggest that the SCF theory underestimates the hydrodynamic size systematically. We note once more that no experimental data below pH = 3.5 are available, and based on calculations discussed above we do not expect many changes below pH 3.5. We thus arrive at the conclusion that the modest size change found by the SCF calculations is in excelent qualitative agreement with the light scattering results.

Experimentally the electrophoretic mobility was measured for these micelles as a function of the amount of acid added to the micelles (i.e. as a function of the pH). This mobility was translated to the ζ potential. It was found that this potential was negative and less negative than −10 mV (i.e., it varied from $\zeta = -7$ to − mV with decreasing pH). In Figure 3d we present the radial electrostatic potential profiles for a series of relevant micelles. Obviously the electrostatic potential is negative throughout the micelles and becomes more negative with increasing pH. In the core the electrostatic potential is significant (it can be as high as −50 mV), but in the corona the value of the electrostatic potential drops rather quickly (this drop will also depend on the ionic strength in the system). We do not exactly know which electrostatic potential is measured in an electrokinetic experiment. In other words, it is uncertain where exactly we should locate the plane of shear. Obviously it is located somewhere inside the corona. The relevant position r where the ζ potential is probed also depends on the micelle size. To facilitate this discussion we give in Figure 4 a few cross-sections of the electrostatic potential at three fixed distances r as indicated. In all cases the electrostatic potential is non-monotonic as a function of pH. For given r the decrease in ζ with pH is due to the increased charge

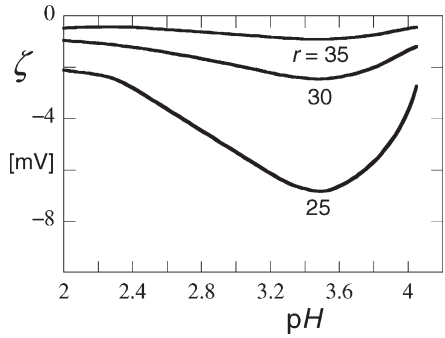

Figure 4.
The electrostatic potential ζ in mV as a function of the pH. The ζ potential is measured at a fixed distance away from the micelle center r as indicated.

density in the core; in a way the surface potential at the core-corona interface increases in magnitude. The subsequent increase of ζ is attributed to the fact that dimensions of the core (and thus the micelle) decreases with pH and one probes the electrostatic potential somewhere in the diffuse part of the electric double layer - where the electrotatic potential drops exponentially-. The non-monotonic ζ potential as presented in Figure 4 thus does not directly mean that the ζ potential measured for these micelles should be non-monotonic with pH. For example, for the condition of pH = 3, the $r = 35$ curve is more relevant, whereas for pH = 4 the $r = 25$ curve should apply. Thus, taking into account that the micelle size decreases with increasing pH, we basically reproduce the trend for the experimental ζ potentials as reported in ref. 17 namely that it increases in size with increasing pH. Important as well is the observation that the order of manitude of the ζ-potential is correct.

With a very reasonable parameter set we are able to reproduce many experimental findings for micelles composed of PMAA-PEO copolymers in aqueous solutions. The non-classical mechanisms of both the driving force and the stopping mechanism as proposed by Konak and Sedlad,[17] which are mimicked by our parameters, are thus confirmed.

Conclusions

In this paper we modeled the formation of micelles composed of PMAA-PEO block copolymers, in the case that the PEO block length is significantly larger than the PMAA block using the self-consistent field theory. We followed the suggestions of Konak and Sedlad[17] that intrachain H-bonding between the proton donor PMMA and the proton acceptor PEO is responsible for the driving force for micellisation. The H-bonding was modeled by inserting a strong negative value for the Flory-Huggings parameter. The length of the PEO block was much longer than the PAA block and the surplus of PEO resulted in the formation of a corona which stopped the micellisation. Our predictions follow the experimental finding semi-quantitatively for all reported quantities such as the aggregation number, the hydrodynamic radius, the ζ potential as a function of the pH. We therefor conclude that the arguments of Konak and Sedlad about the driving force and stopping mechanism for the micellisation are correct. The prediction that the concentration EO in the core is twice that of the MAA may be an interesting target for experimental verification (e.g. by neutron scattering).

[1] D. F. Evans, H. Wennerström, *The Colloidal Domain where physics, Chemistry, Biology and Technnology Meet*, VCH Publishers, NY **1994**.
[2] C. Tanford, *The hydrophobic Effect. Formation of Micelles and Biolocial Membranes*, 2nd ed. , Wiley, **1980**.
[3] S. Alexander, *J. de Phys. Fr.* **1977**, *38*, 983.
[4] P.-G. de Gennes, *Macromolecules* **1980**, *13*, 1096.
[5] T. Cosgrove, T. Heath, B. van Lent, F. Leermakers, J. Scheutjens, *Macrolecules* **1987**, *20*, 1692.
[6] A. N. Semenov, *Sov. Phys. JETP* **1985**, *61*, 733.
[7] S. T. Milner, T. A. Witten, M. E. Cates, *Macromolecules.* **1988**, *21*, 2610.
[8] A. M. Skvorsov, Iv. Pavlushkov, A. A. Gorbunov, E. B. Zhulina, O. V. Borisov, V. A. Priamitsyn, *Pol. Sci. USSR* **1988**, *30*, 1706.
[9] J. Sprakel, N. A. M. Besseling, F. A. M. Leermakers, M. A. Cohen Stuart, *J. phys. Chem. B* **2007**, *111*, 2903.
[10] J. N. Israelachvili, D. J. Mitchell, B. W. Ninham, *J. Chem. Soc. Faraday Trans II* **1976**, *72*, 1525.
[11] F. A. M. Leermakers, C. M. Wijmans, G. J. Fleer, *Macromolecules* **1995**, *28*, 283434.
[12] H. G. Bungenberg de Jong, H. R. Kruyt, *Proceedings of the Koninklijke Nederlandse Akademie van Wetenschappen* **1929**, *32*, 849.
[13] S. van der Burgh, A. de Keizer, M. A. Cohen Stuart, *Langmuir* **2004**, *20*, 1073.
[14] I. K. Voets, A. de Keizer, M. A. Cohen Stuart, *Advances in Colloid and Interface Sci.* **2008**, in press.
[15] A. Harada, K. Kataoka, *Macromolecules* **1995**, *28*, 5294.
[16] Y. Yan, N. A. M. Besseling, A. de Keizer, A. T. M. Marcelis, M. Drechsler, M. A. Cohen Stuart, *Angew. Chem. Int.* **2007**, *46*, 1807.
[17] C. Konak, M. Sedlak, *Macromol. Chem. phys.* **2007**, *208*, 1893.
[18] G. J. Fleer, M. A. Cohen∼Stuart, J. M. H. M. Scheutjens, T. Cosgrove, B. Vincent, *Polymers at Interfaces*, Chapman and Hall, London **1993**.
[19] F. A. M. Leermakers, J. M. H. M. Scheutjens, J. Lyklema, *Biophys. Chem.* **1983**, *18*, 353.
[20] F. A. M. Leermakers, J. M. H. M. Scheutjens, *J. Chem. Phys.* **1988**, *89*, 3264.
[21] K. A. Cogan, F. A. M. Leermakers, A. P. Gast, *Langmuir* **1992**, *8*, 429.
[22] L. A. Meijer, F. A. M. Leermakers, J. Lyklema, *J. Chem. Phys.* **1999**, *110*, 6560.
[23] S. M. Oversteegen, F. A. M. Leermakers, *Phys. Rev. E* **2000**, *62*, 8453.
[24] J. M. P. van den Oever, F. A. M. Leermakers, G. J. Fleer, V. A. Ivanov, N. P. Shusharina, A. R. Khokhlov, P. G. Khalatur, *Phys. Rev. E* **2002**, *65*, 041708.
[25] A. L. Rabinovich, P. O. Ripatti, N. K. Balabaev, F. A. M. Leermakers, *Phys. Rev. E* **2003**, *67*, 011909.
[26] Y. Lauw, F. A. M. Leermakers, M. A. Cohen Stuart, O. V. Borisov, E. B. Zhulina, *Macromolecules* **2006**, *39*, 3628.
[27] M. M. A. E. Claessens, B. F. van Oort, F. A. M. Leermakers, F. A. Hoekstra, M. A. Cohen Stuart, *Biophys. J.* **2004**, *87*, 3882.
[28] R. A. Kik, F. A. M. Leermakers, J. M. Kleijn, *Phys. Chem. Chem. Phys.* **2005**, *7*, 1996.
[29] A. B. Jodar-Reyes, F. A. M. Leermakers, *Physical Chemistry B* **2006**, *110*, 18415.
[30] M. Charlaganov, O. V. Borisov, F. A. M. Leermakers, *Macromolecules* **2008**, *41*, 3668.
[31] R. Israëls, F. A. M. Leermakers, G. J. Fleer, *Macromolecules* **1994**, *27*, 3087.
[32] O. A. Evers, J. M. H. M. Scheutjens, G. J. Fleer, *Macromolecules* **1990**, *23*, 5221.
[33] D. G. Hall, B. A. Pethica, *Non-ionic Surfactants*, Chapter 16, Marcel Dekker, **1976**.

